Journal of the European Ceramic Society 18 (1998) 1307–1312

PII: S0955-2219(98)00058-2
0955-2219/98/$—see front matter

Preparation and Characterization of Dispersed Ruthenium Metal Supported on ex-Boehmite γ-Alumina

Estrella Escalona Platero,[a]* Francisco Ruiz de Peralta[a] and José B. Parra[b]

[a]Departamento de Química, Universidad de las Islas Baleares, 07071 Palma de Mallorca, Spain
[b]Instituto Nacional del Carbón, CSIC, La Corredoria s/n, Ap 73, 33080 Oviedo, Spain

Abstract

$Ru_3(CO)_{12}$ supported on hydroxylated γ-Al_2O_3 by an impregnation procedure was found to decompose into several subcarbonylic species; mainly $Ru^{2+}(CO)_2$, $Ru^0(CO)_2$ and $Ru_3{}^{n+}(CO)_6$, as revealed by FTIR spectroscopy. $Ru^{2+}(CO)_2$ is a mononuclear species, $Ru^0(CO)_2$ contains Ru–Ru bonds and $Ru_3{}^{n+}(CO)_6$ probably retains the triangular Ru_3 skeleton. Thermal decomposition at 773 K in a dynamic vacuum causes decarbonylation of the supported species and formation of small metal aggregates. Part of the metal is oxidized and the rest remains as zerovalent without the need for reduction treatments. The particle size distribution of the metal aggregates shows a maximum at 3·5 nm, as determined by transmission electron microscopy.

1 Introduction

The initial interest of studying supported metal clusters as heterogenized homogeneous catalytic systems[1–4] has been expanded, and nowadays interest is also focused on the use of the supported clusters as precursors of metallic catalysts and metallic thin films. For example, it is known that metal carbonyls provide a convenient route to highly dispersed low-valent metals, without the need for strong reduction treatments.[5–10]

Supported ruthenium is one of the most important active catalysts for CO hydrogenation,[11] being very selective in the production of long chain hydrocarbons.[12] Its catalytic behaviour is affected by the degree of metal dispersion, and by the nature of the support; the presence of promotors can also be important.[12–14] Transition aluminas are among the most extensively used catalyst supports. The relevant factors that determine the adsorptive and catalytic properties, such as crystal structure, surface area and porous texture, and the chemical nature of the surface are largely determined by the precursor material used and the thermal treatment adopted.

We report on a detailed characterization by infrared (IR) spectrometry of $Ru_3(CO)_{12}$ deposited by impregnation onto boehmite-derived γ-Al_2O_3, and on the subsequent thermal decarbonylation to generate supported ruthenium metal which was characterized by IR spectrometry of adsorbed carbon monoxide and by transmission electron microscopy (TEM); the metal charge selected was 5% in weight. Attention was also focused on the morphology and textural parameters of the alumina support, and on the changes it undergoes during the impregnation process and the thermal decarbonylation of the supported metal carbonyl. Previous IR work on $Ru_3(CO)_{12}$ deposited on γ-Al_2O_3 has shown that the metal carbonyl is altered by interaction with the support,[15–18] and the nature of the species thus formed depends on the preparation method adopted (chemical vapour deposition or impregnation), on the hydration/hydroxylation degree of the alumina surface, and on the surface coverage. Total metal concentration in these previous studies[15–18] was never higher than 2% (w/w).

2 Materials and Methods

High-purity tririutheniumdodecacarbonyl was supplied by Aldrich-Chemie (Steinheim). Synthetic boehmite was prepared following the method described by McIver *et al.*[19] This parent material was calcined at 873 K to yield the γ-Al_2O_3 [hereafter called Al(873) sample] used in the present work; the structure was checked by powder X-ray diffraction.

The Al(873) sample was impregnated with an *n*-hexane solution of $Ru_3(CO)_{12}$, and the solvent

*To whom correspondence should be addressed. Fax: 3471173426.

was eliminated by outgassing at 300 K. The metal charge was 5% in weight, and this sample will hereafter be called Ru5Al(300). This sample was heated at increasing temperatures up to 773 K, in a dynamic vacuum of 10^{-3} Pa, in order to decompose the metal carbonyl and to obtain dispersed ruthenium particles; the corresponding sample will hereafter be called Ru5Al(773).

The textural parameters of samples Al(873) and Ru5Al(773) were determined from the corresponding nitrogen adsorption–desorption isotherms obtained at 77 K, by using an automatic instrument (ASAP 2010, Micromeritics). Morphological studies of the Al(873) sample were carried out with a Hitachi S-530 scanning microscope, while the metal particles of the Ru5Al(773) sample were imaged using a Hitachi H-600 transmission electron microscope.

For infrared studies, the Ru5Al(300) sample in the form of a thin self-supporting wafer (about 0·03 g cm^{-2}) was placed inside a vacuum cell,[20] which allowed *in situ* activation, dosing with CO and acquisition of IR spectra. For activation, the sample wafer was heated (in several steps) in a dynamic vacuum (residual pressure 10^{-3} Pa) for 20 min at increasing temperature from 300 to 773 K. After each activation period, the sample was allowed to cool to room temperature, the evolved CO was evacuated by outgassing the IR cell for a few minutes, and IR spectra were taken. Room temperature IR transmission spectra were recorded, at 3 cm^{-1} resolution, using an FTIR Bruker 66 spectrometer.

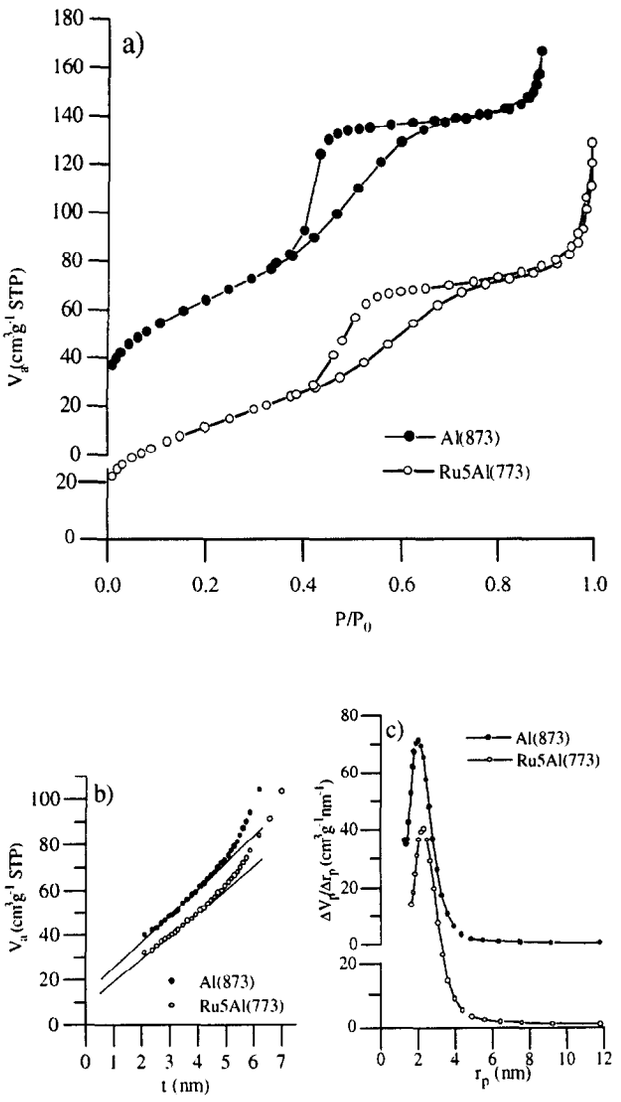

Fig. 1. (a) Nitrogen adsorption–desorption isotherms, at 77 K, on samples Al(873) and Ru5Al(773). (b) Adsorbed volume (V_a) versus multilayer thickness (t) for the same samples. (c) Pore-size distribution curves: r_p = pore radius, V_p = pore volume.

3 Results and Discussion

3.1 Textural and morphological characterization

Nitrogen adsorption–desorption isotherms on samples Al(873) and Ru5Al(773) were obtained after outgassing the samples at 473 K in a dynamic vacuum of 10^{-2} Pa. Both were found to be similar, and akin to type IV (with a small contribution from type I) of the BDDT classification,[21] as shown in Fig. 1a. The hysteresis loops correspond to type H2 of the classification proposed by the IUPAC.[22] These facts suggest that the materials exhibit micro- and mesoporosity.

The presence of microporosity, suggested by the shape of the nitrogen adsorption isotherms, has been confirmed by using the de Boer V_a–t method.[23] Plots of volume of adsorbed nitrogen (V_a) versus multilayer thickness (t) revealed a contribution from microporosity which amounts to 5–10% of the total pore volume (Table 1). This was calculated from the vertical intercept of the corresponding V_a–t plots (Fig. 1b). The V_a–t plots were obtained using the standard isotherms n_1 [for sample Al(873)] and n_2 [for sample Ru5Al(773)] taken from the work of Lecloux and Pirard.[24] These standard isotherms were chosen so as to match the C_{BET} parameter of the experimental isotherms analysed.

BET and t-surface areas were calculated from the corresponding adsorption isotherms and V_a–t plots, respectively, using the value of 0·162 nm^2 for the surface covered by one nitrogen molecule. The results are given in Table 1. Consistent with the presence of microporosity is the fact that the S_{BET} values were considerably larger than the corresponding S_t values. Also shown in Table 1 are the total pore volume (V_p) and the most frequent pore radius (r_p). The pore volume was obtained by multiplying the amount of adsorbed nitrogen, directly read from the isotherms at $P/P_0 = 0{\cdot}9975$, by the conversion factor 0·00156.[25] The most frequent pore radius, in the mesoporous range, was

Table 1. Textural parameters of Al(873) and Ru5Al(773) samples

Sample	S_{BET} $(m^2 g^{-1})$	S_t $(m^2 g^{-1})$	V_p $(cm^3 g^{-1})$	V_{microp} $(cm^3 g^{-1})$	r_p (nm)	%ΣV$_{ads}$ $r_p < 1$ (nm)	$1 < r_p < 25$ (nm)	$r_p > 25$ (nm)
Al(873)	222	180	0·250	0·0218	2	8·54	78·05	13·41
Ru5Al(773)	184	158	0·268	0·0140	2	4·89	65·76	29·35

calculated following the Pierce method[26] with the equation of Halsey for multilayer thickness.[27] The monolayer thickness was taken as 354 pm. The analysis was applied to the adsorption branch of each isotherm, which must be preferred to the desorption branch for type IV isotherms.[28] The pore size distribution curve showed in both cases a maximum at *ca.* 2 nm, (Fig. 1c).

On passing from sample Al(873) to Ru5Al(773) a decrease of surface area and an increase of pore volume was observed (Table 1). This change of textural parameters during the impregnation and decarbonylation procedures can be explained in terms of a sintering process. In fact, there is a decrease of the pore volume in pores of $r_p < 1$ nm from 8·54% down to 4·89%, and a parallel increase of the pore volume in pores of $r_p > 25$ nm from 13·41% up to 29·35%, which suggest a partial collapse of the micropore system and parallel formation of larger particles at the expenses of smaller ones.

Figure 2 is a representative micrograph of the Al(873) sample. The lamellar structure observed suggests a topotactic transformation during the dehydration process of boehmite, since this mineral is known to have a layer structure.

3.2 FTIR characterization

Figure 3 shows the FTIR spectrum of sample Ru5Al(300) in the CO stretching region (spectrum 1) and the subsequent modifications it undergoes when the sample is heated in a vacuum at increasing

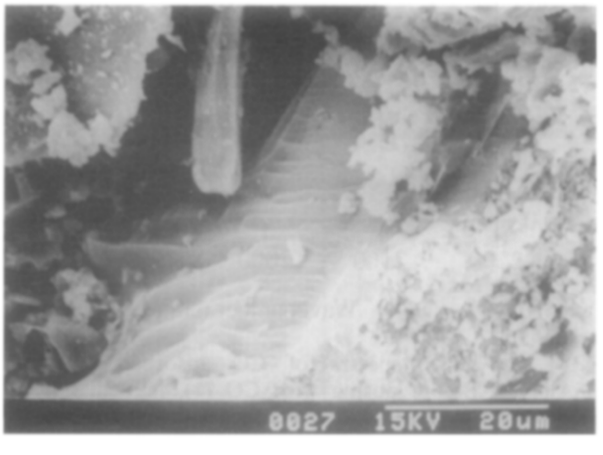

Fig. 2. Representative SEM micrograph of the Al(873) sample.

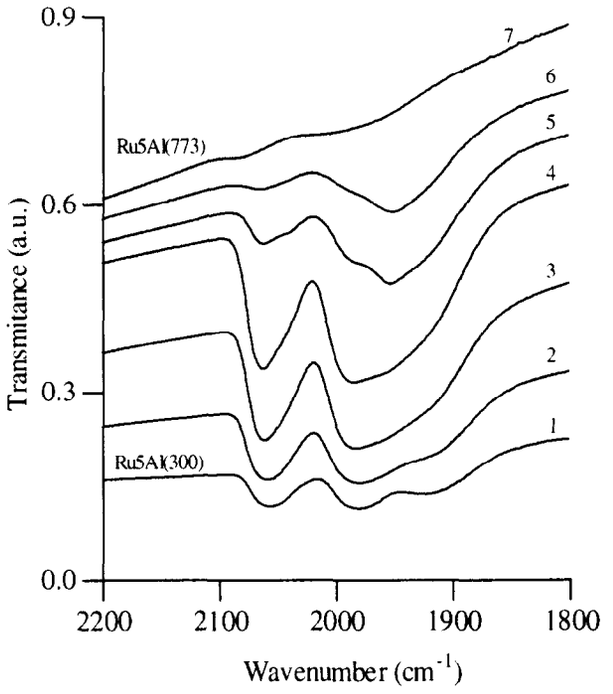

Fig. 3. FTIR spectra of $Ru_3(CO)_{12}$ impregnated on γ-Al_2O_3. Sample Ru5Al(300) (1) and subsequent activation in vacuum for 20 min at 300 (2), 423 (3), 523 (4), 623 (5), 673 (6) and 773 K (7) [sample Ru5Al(773)].

temperatures up to 773 K (spectra 2–7). Spectrum 1 shows three broad absorptions centred at 2060, 1985 and 1915 cm^{-1}. By outgassing at 523 K (spectrum 4), the band centred at 2060 cm^{-1} becomes sharper, shifts to 2067 cm^{-1}, and develops a shoulder at 2040 cm^{-1}. Simultaneously, the other two bands (at 1985 and 1915 cm^{-1}) collapse into a broader absorption with several components; a maximum can be observed at 1992 cm^{-1}, which has a tail on the low frequency side showing shoulders at 1953 and 1915 cm^{-1}. On heating at 623 K (spectrum 5) the overall intensity decreases and the shoulders at 2040 and 1953 cm^{-1} become more prominent. Finally, for the sample fired at 773 K (spectrum 7) the CO stretching bands have almost disappeared. Temperatures higher than 773 K have been discarded in order to avoid severe sintering of the metal particles.

In the range 1650–1300 cm^{-1} (not shown), several bands were also observed, which could be assigned to carbonate-like species formed upon partial decomposition of alumina-supported $Ru_3(CO)_{12}$ [sample Ru5Al(300)]. These species were decomposed upon heating at 773 K.

The IR spectrum of $Ru_3(CO)_{12}$ in CCl_4 solution shows four bands at 2062 (A_2''), 2026 (E'), 2002 (E') and 1989 cm^{-1} (E').[29] Comparing these features with the wavenumbers observed in spectrum 1 of Fig. 3, it can be concluded that $Ru_3(CO)_{12}$ does not retain its molecular structure upon interaction with the alumina surface. The supported metal carbonyl is not simply physisorbed, it undergoes partial decarbonylation; i.e. a process of dissociative chemisorption. Decomposition of alumina-supported ruthenium carbonyl has also been observed previously,[15–18] and the nature of the transformation products depends on several parameters, as already stated in the Introduction.

Zecchina *et al.*[16] have studied two $Ru_3(CO)_{12}/Al_2O_3$ systems where the metal charge was 0·33 and 1·57 wt% and, on the basis of isotopic substitutions, have concluded that $Ru_3(CO)_{12}$ deposited onto hydroxylated γ-Al_2O_3 forms two mononuclear dicarbonylic species, $Ru^{3+}(CO)_2$ (IR bands at 2138 and 2075 cm^{-1}) and $Ru^{2+}(CO)_2$ (2075 and 2005 cm^{-1}), and a zerovalent species $Ru^0(CO)_2$ (main IR bands at 2054 and 1977 cm^{-1}) where metal–metal bonds are preserved. Our IR spectra (Fig. 3) are similar to those described by Zecchina *et al.*, but some differences also exist. Most distinctively, IR bands corresponding to the $Ru^{3+}(CO)_2$ species are not present in our spectra, while an additional band is observed at 1915 cm^{-1}.

Following Zecchina *et al.*,[16] the two broad bands centred at 2060 and 1985 cm^{-1} (Fig. 3) are assigned to $Ru^{2+}(CO)_2$ and $Ru^0(CO)_2$ species. These species evolve in a different way by thermal treatment. During the initial steps of the activation process, IR bands corresponding to the $Ru^0(CO)_2$ species lose intensity, while those corresponding to the $Ru^{2+}(CO)_2$ species (2067 and 1992 cm^{-1}) gain prominence. Since studies of adsorbed CO (see later) have shown the presence of zerovalent ruthenium after firing at 773 K, this spectroscopic evidence suggests progressive decarbonylation of the $Ru^0(CO)_2$ species. The band at 1915 cm^{-1}, not observed by Zecchina *et al.*,[16] is tentatively assigned to CO adsorbed in a linear mode at a ruthenium atom with high electron density, as reported by Kellner and Bell,[30] but no further characterization of the corresponding species can be done on account of the present IR spectra.

The IR bands at 2040 and 1953 cm^{-1} (spectra 4–6, Fig. 3), developed during activation at 523–673 K, are assigned to $Ru_3^{n+}(CO)_6$ ($n = 1$–3) species, which have three terminal and three bridging CO groups. This assignment has been done following Asakura *et al.*,[18] who by using EXAFS spectroscopy have shown that alumina supported $Ru_3^{n+}(CO)_6$ species retain the triangular Ru_3 skeleton of molecular $Ru_3(CO)_{12}$.

At 773 K [sample Ru5Al(773)] the decarbonylation is nearly complete (spectrum 7, Fig. 3). The remaining metal particles were characterized by FTIR spectroscopy of adsorbed CO. Figure 4a shows the spectra obtained immediately after contact with CO (spectrum 2), and the evolution with time (spectra 3–5); Fig. 4b shows the effect of thermal treatments on the carbonylic species formed by interaction with CO (spectra 6–11).

The supported metal particles on the surface of sample Ru5Al(773) are able to coordinate CO at

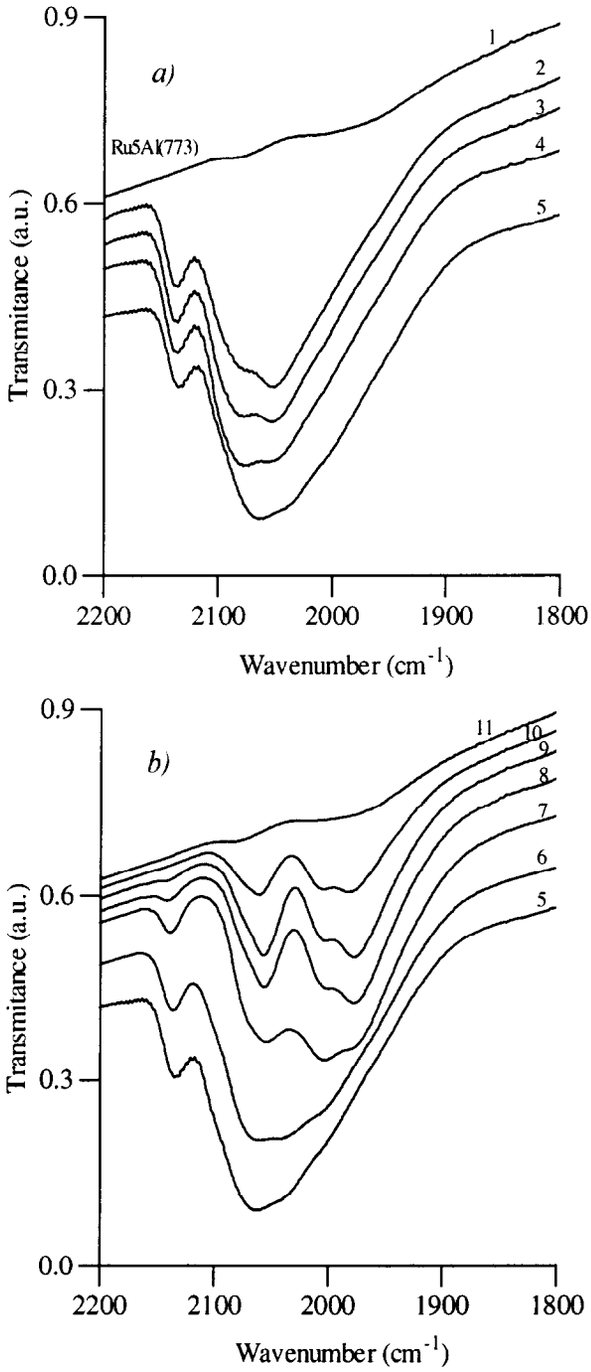

Fig. 4. (a) FTIR spectra of CO adsorbed on sample Ru5Al(773). Before dosing with CO (1), immediately after dosing with CO (2), and after contact with CO for 5 min (3), 2 h (4) and 15 h (5). (b) Last spectrum in Fig. 4a (spectrum 5), and effect of heating in vacuum for 10 min at 300, 400, 450, 500, 573 and 673 K: spectra 6–11.

room temperature, as shown in Fig. 4a. Spectrum 2 shows a low intensity band at 2138 cm^{-1}, and a broad absorption with two maxima at 2083 and 2053 cm^{-1}, together with a long tail in the low frequency side. Prolonged exposure of the sample to adsorbed CO results in an overall intensity growth of the IR spectra (spectra 3–5, Fig. 4a) and an inversion of the relative intensity of bands at 2083 and 2053 cm^{-1}, which indicates that these bands do not correspond to the same chemical species. The intensity growth suggests disruption of the metal particles with formation of low-nuclearity anchored carbonylic species.[16,31] According to Zecchina *et al.*,[16] the bands at 2138 and 2083 cm^{-1} are assigned to dicarbonylic species $Ru^{3+}(CO)_2$, while the band at 2053 cm^{-1} corresponds to CO adsorbed on zerovalent ruthenium.

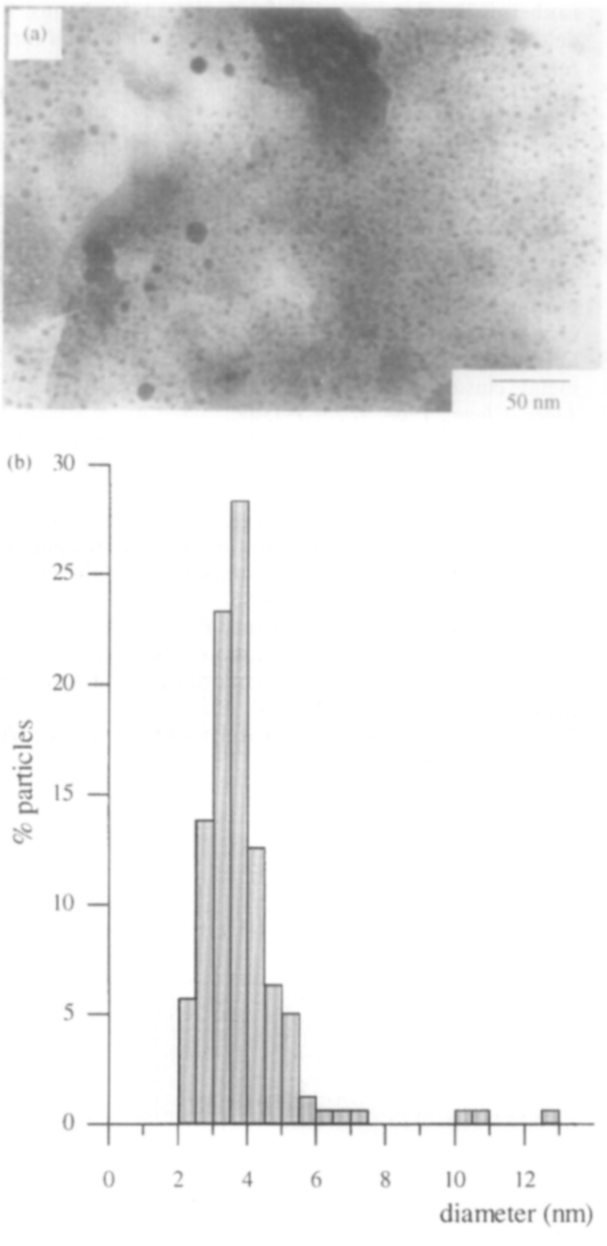

Fig. 5. (a) Representative TEM micrograph of the Ru5Al(773) sample. (b) Metal particle size distribution.

Zerovalent metallic aggregates were also identified during thermal treatments at increasing temperature. Thus, in Fig. 4b, the bands at 2053 and 1975 cm^{-1} are assigned to a zerovalent ruthenium dicarbonylic species: $Ru^0(CO)_2$,[16,17] and the band at 2007 cm^{-1} was assigned to a zerovalent ruthenium monocarbonylic species: Ru^0-CO.[30,32] After thermal treatment at 673 K (spectrum 11) subsequent exposure to CO (spectra not shown) lead to reproduction of the IR spectra in Fig. 4a, thus showing reversibility of the decarbonylation/carbonylation process.

Figure 5a shows a representative TEM micrograph of sample Ru5Al(773). The metal particles (high optical density spots) have a spherical shape and a rather narrow size distribution. The results of statistical analysis are shown in Fig. 5b; most metal aggregates have a diameter in the 1–5 nm range, with a sharp maximum at ca 3·5 nm. Supported metal particles of these dimensions have been shown[33] to be of paramount interest for many catalytic processes.

4 Conclusions

$Ru_3(CO)_{12}$ supported on hydrated γ-Al_2O_3 by an impregnation procedure has been studied by FTIR spectroscopy. The IR spectra revealed that on interaction with the support the metal carbonyl decomposes into several subcarbonylic species; mainly $Ru^{2+}(CO)_2$, $Ru^0(CO)_2$ and $Ru_3{}^{n+}(CO)_6$. These species can be further decarbonylated by heating in a vacuum at 773 K, with formation of dispersed metal particles. FTIR spectra of adsorbed CO on these metal particles have indicated that although part of the metal ruthenium is oxidized (probably to Ru^{3+}) a substantial part forms zerovalent ruthenium aggregates which are 1–5 nm in diameter, as shown by transmission electron microscopy. These results show that the method used affords a convenient route for preparing catalytically useful materials.

Acknowledgements

This research was supported by the Spanish DGICYT, Ref. PB93-0425. The authors thank Professor C. Otero Areán for helpful discussions and Dr F. Hierro Riu for obtaining the electron micrographs.

References

1. Bailey, D. C. and Langer, S. H., Immobilised transition-metal carbonyls and related catalysts. *Chem. Rev.*, 1981, **81**, 109–148.

2. Ozin, G. A. and Gil, C., Intrazeolite organometallics and coordination complexes: internal versus external confinement of metal guests. *Chem. Rev.*, 1989, **89**, 1749–1764.
3. Zecchina, A. and Otero Areán, C., Structure and reactivity of surface species obtained by interaction of organometallic compounds with oxidic surfaces: IR studies. *Catal. Rev.*, 1993, **35**, 261–315.
4. Ugo, R., Dossi, C. and Psaro, R., Molecular metal carbonyl clusters and volatile organometallic compounds for tailored mono and bimetallic heterogeneous catalysts. *J. Mol. Catal.*, 1996, **107**, 13–22.
5. Whyman, R., Industrial aspects of cluster chemistry. *Phil. Trans. R. Soc. Lond. A*, 1982, **308**, 131–140.
6. Asakura, K. and Iwasawa, Y., Surface structure and catalysis for CO hydrogenation of the supported Ru species derived from the $Ru_3(CO)_{12}$ inorganic oxides. *J. Chem. Soc. Faraday Trans.*, 1990, **86**, 2657–2662.
7. Escalona Platero, E., Ruiz de Peralta, F. and Otero Areán, C., Vapour phase deposition and thermal decarbonylation of $Re_2(CO)_{10}$ on gamma-alumina: infrared studies. *Catal. Lett.*, 1995, **34**, 65–73.
8. Gates, B. C., Supported metal clusters: synthesis, structure, and catalysis. *Chem. Rev.*, 1995, **95**, 511–522.
9. Mas Carbonell, C. and Otero Areán, C., Adsorption and thermal decarbonylation of $Re_2(CO)_{10}$ on high-surface-area spinel: infrared studies. *Vib. Spectrosc.*, 1996, **12**, 103–107.
10. Boyd, E. P., Ketchum, D. R., Deng, H. and Shore, S. G., Chemical vapor deposition of metallic thin films using homonuclear and heteronuclear metal carbonyls. *Chem. Mater.*, 1997, **9**, 1154–1158.
11. Vannice, M. A., Catalytic synthesis of hydrocarbons from hydrogen–carbon monoxide mixtures over the group VIII metals. *J. Catal.*, 1975, **37**, 449–461.
12. Okuhara, T., Kimura, T., Kobayashi, K., Misono, M. and Yoneda, Y., Effects of dispersion in carbon monoxide adsorption and carbon monoxide hydrogenation over alumina-supported ruthenium catalysts. *Bull. Chem. Soc. Jpn.*, 1984, **57**, 938–943.
13. King, D. L., A Fischer–Tropsch study of supported ruthenium catalysts. *J. Catal.*, 1978, **51**, 386–397.
14. Kellner, C. S. and Bell, A. T., Effects of dispersion on the activity and selectivity of alumina-supported ruthenium catalysts for carbon monoxide hydrogenation. *J. Catal.*, 1982, **75**, 251–261.
15. Kuznetsov, V. L., Bell, A. T. and Yermakov, Y., An infrared study of alumina- and silica-supported ruthenium cluster carbonyls. *J. Catal.*, 1980, **65**, 374–389.
16. Zecchina, A., Guglielminotti, E., Bossi, A. and Camia, M., Surface characterization of $Ru_3(CO)_{12}/Al_2O_3$ system. I. Interaction with the hydroxylated surface. *J. Catal.*, 1982, **74**, 225–239. II. Structure and reactivity of the surface carbonylic complexes. *J. Catal.*, 1982, **74**, 240–251. III. Surface properties after full decarbonylation and reduction. *J. Catal.*, 1982, **74**, 252–265.
17. Beck, A., Dobos, S. and Guczi, L., Reactivity of surface intermediates derived from Al_2O_3-supported $Ru_3(CO)_{12}$ in the $CO+H_2$ reaction. *Inorg. Chem.*, 1988, **27**, 3220–3226.
18. Asakura, K., Bando, K.-K. and Iwasawa, Y., Structure and behaviour of $Ru_3(CO)_{12}$ supported on inorganic oxide surfaces, studied by EXAFS, infrared spectroscopy and temperature-programmed decomposition. *J. Chem. Soc. Faraday Trans.*, 1990, **86**(CO), 2645–2655.
19. McIver, D. S., Tobin, H. H. and Barth, R. T., Catalytic aluminas. I. Surface chemistry of eta and gamma alumina. *J. Catal.*, 1963, **2**, 485–497.
20. Boccuzzi, F., Coluccia, S., Ghiotti, G. and Zecchina, A., Infrared study of surface modes on silica. *J. Phys. Chem.*, 1978, **82**, 1298–1303.
21. Brunauer, S., Deming, L. S., Deming, W. S. and Teller, E., On a theory of the van der Waals adsorption of gases. *J. Am. Chem. Soc.*, 1940, **62**, 1723–1732.
22. Sing, K. S. W., Everett, D. H., Haul, R. A. W., Moscou, L., Pierotti, R. A., Rouquérol, J. and Siemieniewska, T., Reporting physisorption data for gas/solid systems. *Pure Appl. Chem.*, 1984, **57**, 603–619.
23. Lippens, B. C. and de Boer, J. H., Studies on pore systems in catalysts V. The t method. *J. Catal.*, 1965, **4**, 319–323.
24. Lecloux, A. and Pirard, J. P., The importance of standard isotherms in the analysis of adsorption isotherms for determining the porous texture of solids. *J. Colloid Interface Sci.*, 1979, **70**, 265–281.
25. Sing, K. S. W., Assesment of microporosity. *Chem. Ind.*, 1967, 829–830.
26. Pierce, C. J., Computation of pore sizes from physical adsorption data. *J. Phys. Chem.*, 1953, **57**, 149–152.
27. Halsey, G. D., Physical adsorption on nonuniform surfaces. *J. Chem. Phys.*, 1948, **16**, 931–937.
28. Mata Arjona, A., Parra Soto, J. B. and Otero Areán, C., Analysis of nitrogen adsorption–desorption isotherms on porous metal oxides: a comparative study of several models. *Stud. Surf. Sci. Catal.*, 1982, **10**, 175–186.
29. Quicksall, C. O. and Spiro, T. G., Raman frequencies of metal cluster compounds: $Os_3(CO)_{12}$ and $Ru_3(CO)_{12}$. *Inorg. Chem.*, 1968, **7**, 2365–2369.
30. Kellner, C. S. and Bell, A. T., Infrared studies of carbon monoxide hydrogenation over alumina-supported ruthenium. *J. Catal.*, 1981, **71**, 296–307.
31. Mizushima, T., Tohji, K., Udagawa, Y. and Ueno, A., EXAFS study of the CO-adsorption-induced morphology change in ruthenium clusters supported on alumina. *J. Phys. Chem.*, 1990, **94**, 4980–4985.
32. Pfnür, H., Menzel, D., Hoffmann, F. M., Ortega, A. and Bradshaw, A. M., High resolution vibrational spectroscopy of CO on Ru(001): the importance of lateral interactions. *Surf. Sci.*, 1980, **93**, 431–452.
33. Boudart, M., Heterogeneous catalysis by metals. *J. Mol. Catal.*, 1985, **30**, 27–38.